

Dalton Transactions

Conductance Fluctuations in Cobalt Valence Tautomer Molecular Thin Films

Journal:	Dalton Transactions
Manuscript ID	DT-ART-08-2024-002213.R1
Article Type:	Paper
Date Submitted by the Author:	21-Sep-2024
Complete List of Authors:	Phillips, Jared; Indiana University Indianapolis, Physics Yazdani, Saeed; Indiana University Indianapolis, Department of Physics Soruco, Joseph; Indiana University Indianapolis Oles, Jackson; Indiana University Indianapolis Ekanayaka, Thilini; University of Nebraska-Lincoln, Physics Mishra, Esha; University of Nebraska - Lincoln, Physics and Astronomy Wang, Ping; Florida State University Zaz, Zaid; University of Nebraska-Lincoln Liu, Jing; Purdue University System N'Diaye, Alpha; Lawrence Berkeley National Laboratory, Advanced Light Source Shatruk, Michael; Florida State University, Department of Chemistry and Biochemistry Dowben, Peter; University of Nebraska - Lincoln, Physics and Astronomy Cheng, Ruihua; Indiana University Indianapolis, Physics

SCHOLARONE™ Manuscripts

ARTICLE

Received 00th January 20xx, Accepted 00th January 20xx

DOI: 10.1039/x0xx00000x

Conductance Fluctuations in Cobalt Valence Tautomer Molecular Thin Films

Jared P. Phillips, ^a Saeed Yazdani, ^a Joseph Soruco, ^a Jackson Oles, ^a Thilini K. Ekanyaka, ^b Esha Mishra, ^b Ping Wang, ^c M. Zaid Zaz, ^b, Jing Liu, ^a, Alpha T N'Diaye, ^d Michael Shatruk, ^c Peter A. Dowben, *^b Ruihua Cheng *^a

Abstract: The conductivity changes associated with optical excitations and changing temperature, in cobalt valence tautomer molecular thin films were investigated. Conductance switching in the presence of illumination is observed, with occasional locking in a higher conductance state, depending on the temperature, the photon energy of the illumination, and the bias voltage. Light of sufficiently short wavelengths is needed to ensure the light enhanced conductance switching, consistent with the optical absorption, but bias voltage clearly plays a role as well. The conductance switching is associated with excitations to the ligand to metal charge transfer state.

Introduction

Spin crossover (SCO) and valence tautomeric (VT) complexes are two similar classes of molecules exhibiting a bistability between a low spin (LS) and a high spin (HS) state. They can be switched between these two states by a number of external stimuli, including temperature, light irradiation, pressure, magnetic field, and electric field, ¹⁻⁸ making these materials attractive candidates for next generation molecular based electronics. ⁹⁻²² Each state possesses distinct physical properties, with one of the most intriguing being the spin state dependent electrical conductivity. ⁹⁻²¹

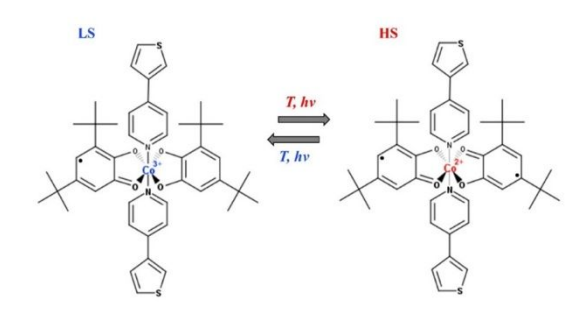


Figure 1. The valence tautomeric low spin (LS) and high spin (HS) forms of [Co(SQ)(Cat)(3-tpp)2].

The spin state switching phenomenon arises in transition metal coordination complexes due to the energy splitting of the five 3d orbitals of metal ions into t_{2g} and e_g levels. For valence tautomer complexes, the conversion between the LS and HS states is associated with electron charge transfer between redox-active ligands and the metal center. 22-39 For an octahedral cobalt complex, the LS Co(III) state, shown in Figure 1, has an electronic configuration t_{2g}^6 , S = 0, ${}^{1}A_{1}$. After an intramolecular electron charge transfer from ligand to Co(III) metal ion, it becomes the paramagnetic HS state Co(II) species with $t_{2g}^5 e_g^2$, S = 3/2, ⁴T₂, with a concomitant change in the oxidation and spin state of the redox-active ligand (see below). These complexes are often highly sensitive to light irradiation, 29-37 X-rays 38-40 or the X-ray generated secondary electrons. The valence tautomer transition can lead to a change in conductivity, 22 similar to the SCO complexes. 9-21 The direct photoinduced spin state change is optically forbidden. Frequently for many molecular spin crossover complexes the photoinduced LS-to-HS switching proceeds through direct spin-allowed excitation to a ligandmetal charge transfer (LMCT) state, followed by a decay into the metastable HS state. 41,42 Such LMCT states have been identified recently for the valence tautomer complex [Co^{II}(SQ)₂(3-tpp)₂].⁴³ The question is whether under an applied electric field the photoinduced spin state change is hindered or enhanced.

In this paper, we report a study on the temperature, light, and bias voltage dependent valence tautomer transition from the LS $[Co^{III}(SQ)(Cat)(3-tpp)_2]$ (3-tpp = 3-thienylpyridine) to the HS $[Co^{III}(SQ)_2(3-tpp)_2]$, as illustrated in Figure 1, where Cat = 3,5-di-tert-butylcatecholate (S = 0) and SQ = 3,5-di-tert-butylsemiquinonate (S = 1/2). These particular complexes exhibit a change in spin state between 300 K and 400 K, associated with a valence tautomer transition centered about 370 K.^{43,44} Prior work on the electronic structure of $[Co^{III}(SQ)(Cat)(3-tpp)_2]$ and $[Co^{III}(SQ)_2(3-tpp)_2]$ indicates that

^a Department of Physics, Indiana University-Purdue University Indianapolis, Indianapolis, Indiana 46202, USA.

b. Department of Physics and Astronomy, Jorgensen Hall, University of Nebraska, Lincoln, NE 68588-0299, USA.

^c Department of Chemistry and Biochemistry, Florida State University, 95 Chieftain Way, Tallahassee, FL 32306, USA.

^d Advanced Light Source, Lawrence Berkeley National Laboratory, Berkeley, CA 94720, USA.

optical excitations to the HS state would require a photon energy between 2.8 and 3.7 $\,\mathrm{eV^{43}}$ to ensure an excitation to the LMCT state, which could then subsequently decay to the high spin state. 41,42 If the photon energy is too small, excitations to largely Cat- and 3-tpp- weighted molecular orbitals are forbidden by symmetry selection rules, resulting to the low optical absorption cross-section. 43

Experimental Methods

The synthesis of $[Co(SQ)(Cat)(3-tpp)_2]$ (3-tpp = 3-thienylpyridine) was carried out by layering a solution of $[Co^{II}(SQ)_2]_4$ (270 mg, 0.13 mmol) in 8 mL of toluene on top of a solution of 3-tpp (172 mg, 1.07 mmol) in 5 mL of dichloromethane, which led to the formation of blue crystals after a few weeks. The crystals were recovered by filtration, washed with toluene, and dried under vacuum at 100 °C for 24 h, resulting in a dark powder with a yield of 180 mg (42%), as described previously in details.⁴⁴

Thin film samples were prepared using drop casting. Solutions of $[Co(SQ)(Cat)(3-tpp)_2]$ were created by dissolving 1 mg of the complex (weighed using an AG 104 analytical balance) in 3 mL of toluene. Various other solvents, including dichloromethane, acetone, and methanol, were tested. The best solubility was achieved in toluene, while also minimizing the "coffee ring" drying effect. ⁴⁵ The solutions were sonicated for 20 min followed by stirring using a vortex mixer.

The approximate thickness of the thin films prepared by each drop cast can be determined by the relation, $t=\frac{V_C}{A}$, where t is the thickness of the film, V_C is the volume of solute contained in a single drop of the drop-cast solution, and A is the total area fully covered by a drop of the solution. For samples used in X-ray absorption spectroscopy (XAS) and ultravioletvisible (UV-Vis) spectroscopy studies, each drop of solution drawn from the pipette is 25 μ L and it covers the substrate's surface area of approximately 1 cm². Using a solute-to-solvent volume ratio of 0.0009 mL of [Co(SQ)(Cat)(3-tpp)₂] powder (ρ = 1.1 g/cm³) to 3 mL of toluene (ρ = 0.867 g/cm³), a single drop, with V_C = 1.5 × 10-6 mL, created a thin film of [Co(SQ)(Cat)(3-tpp)₂] with a nominal thickness of 75 nm. All the spectra are normalized by the maximum peak for better comparison.

The samples for electron transport studies were prepared using gold interdigitated electrodes (IDEs) (Figure S1) purchased from Micrux Technologies.²⁰ For this purpose, thin films of $[Co(SQ)(Cat)(3-tpp)_2$ were prepared on interdigitated electrodes and mounted on a custom-built variable temperature transport measurement stage, connected via silver painted gold wire electrodes. Initial background conductance readings were performed on a bare interdigitated electrode chip to ensure adequately clean interdigitated electrodes without contamination or chip defects. A picoampmeter reading below the range of 1×10^{-12} A indicated a sufficiently clean substrate. Next, a 250 nm thick molecular film was deposited via drop casting onto the interdigitated electrode substrate and allowed to dry under vacuum. The interdigitated electrodes consisted of an electrode pair

arranged in a zigzag path and spanning an equivalent length of 1 m, a height of 200 nm (50 nm Ti beneath 150 nm Au) and separated by a 5-micron gap. The drop cast of [Co(SQ)(Cat)(3-tpp)₂] solution covers a surface area of each interdigitated electrode pattern, $^{\sim}$ 0.5 cm², requiring 10 individual 5- μ L drops ($^{\sim}$ 30 nm thickness per drop) for optimal functionality. The transport measurements data acquisition was done by collecting the individual I(V) curves as a function of temperature. These data were then converted to the conductance, using the information on the cross-section area between two electrodes. The raw data are provided in the supplementary materials (Figure S2).

While the choice of substrate can certainly affect the spin state of a spin crossover thin film, in the thin film limit,⁴⁶ the glass substrate of the gold interdigitated electrodes used here does not seem to affect the spin state transition of the $[Co^{\parallel}(SQ)(Cat)(3-tpp)_2]/[Co^{\parallel}(SQ)_2(3-tpp)_2]$ thin films. In fact, the electronic structure of [Co^{III}(SQ)(Cat)(3-tpp)₂]/[Co^{II}(SQ)₂(3tpp)2] has been found to be surprisingly insensitive to a wide range of substrates.⁴³ As indicated here, this is influenced by the electric polarization of the organic ferroelectric polyvinylidene fluoride-hexafluoropropylene (PVDF-HFP). PVDF-HFP thin films were deposited using a lab-built Langmuir-Blodgett (LB) machine, as described elswhere. 12,20,47 To achieve an optimal β phase in PVDF-HFP, thin films were annealed and postannealing, a 300 nm film of $[Co^{\parallel}(SQ)(Cat)(3-tpp)_2]/[Co^{\parallel}(SQ)_2(3-tpp)_2]$ tpp)₂] film was added. To obtain the desired polarity of the PVDF-HFP layer, a negative or positive voltage of 30 V was applied for 30 seconds then the bias voltage was gradiually decreased back to zero. The UV-Vis measurements were done several times on multiple samples and similar results were acquired.

Charge transport measurements were conducted under vacuum using a custom-built and fully automatic controlled variable temperature stage. 20,47 This is important as an I(V) curve transport measurement is acquired slowly (5 minutes for a full sweep), which combined with the time taken for each temperature to stabilize, a full temperature dependent measurement cycle is acquired in about 10 hours. XAS experiments were carried out at the magnetic spectroscopy beamline 6.3.1 of Advanced Light Source (ALS) at Lawrence Berkeley National Lab in Berkeley, California. The measurements were taken in the total electron yield (TEY) mode, indicating that the XAS measurements were surface sensitive. The photon flux was approximately ${\sim}10^{11}$ photons/sec, as described in other studies. 12,20,39,43 UV-Vis spectrometry measurements were performed using a Thermo-Fisher Scientific G10S UV-Vis spectrometer equipped with a custom-developed sample heater (parts purchased from Thermo-Fisher Scientific Inc., Waltham, Massachusetts, USA).43,47

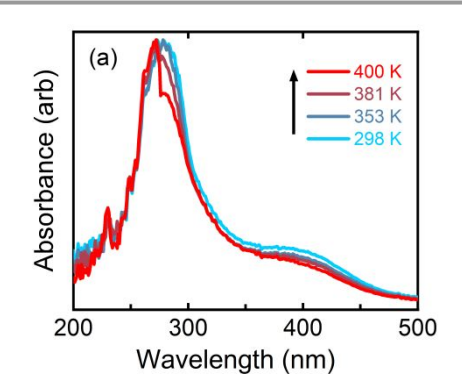
Identification of the Ligand to Metal Charge Transfer State

The key focus of this paper is the conductance fluctuations. Inverse photoemission, X-ray absorption (XAS) and optical measurements have been compared to better explain the effect of optical excitations on the conductance, as discussed below. The temperature dependent Co-L₃ and L₂ XAS spectra (Figure S3), recorded for a thin film of [Co(SQ)(Cat)(3-tpp)₂] with a thickness of around 75 nm prepared on a HOPG substrate, show minor changes as the temperature increases from 300 K to 390 K. For the HS form, $[Co^{II}(SQ)_2(3-tpp)_2]$, both e_g and t_{2g} orbitals are partially occupied, as indicated with peaks at 775.9 eV and 777.3 eV corresponding to the excitations to t_{2g} orbitals and e_g orbitals, respectively. There may be a slight decrease in the intensity of the 777.3 eV feature, as the temperature increases, but in general the XAS does not change much with temperature, especially with decreasing temperature. It is clear from the XAS that the [Co(SQ)(Cat)(3-tpp)₂] film is largely in the HS states under the X-ray fluence, as previously noted.⁴³

All the XAS spectra (Figure S1(b)) collected with decreasing temperature from 390 K to 300 K show negligible differences, suggesting that the more complete spin state conversion achieved on heating is sustained for a single heating and cooling cycle, i.e., the spin state becomes locked in the film after subjected to thermal treatment, when under continuous X-ray flux. This locking could be due to several factors, mainly the previously mentioned photo-active nature of many Co valence tautomer molecules, 29-40 including X-ray 38-40 trapping the $[Co^{\parallel}(SQ)(Cat)(3-tpp)_2]$ or $[Co^{\parallel}(SQ)_2(3-tpp)_2]$ metastable state,⁴⁰⁻ 42 possibly sustained due to the incident X-ray flux and secondary electron generation (although reversible over many subsequent heating and cooling cycles). Another possibility is temperature, and possibly X-ray fluence, induced changes in the packing of molecules in the thin film, which could lead to a change in the ratio of the HS and LS molecules. 41 Similar effects are seen with temperature, and illumination closer to the visible

The UV-Vis spectra measured on the thin film of [Co(SQ)(Cat)(3-tpp)₂] in the wavelength range of 200-800 nm also indicate a transition with increasing temperature (Figure 2a) and a locked state with negligible change in spectra upon decreasing the temperature (Figure 2b). Figure 2a shows the UV-Vis optical absorption spectra of a 75 nm thin film of [Co(SQ)(Cat)(3-tpp)₂] on a glass substrate taken during the initial temperature ramp from 298 K to 400 K. The absorbance peak near 270 nm gradually increases as temperature rises, while the absorbance peaks near and 400 nm and 280 nm decrease, but these changes to the optical absorption are relatively small, especially with decreasing temperatures. These characteristic optical transitions from the highest occupied molecular orbital (HOMO) to the various unoccupied molecular orbitals, show a narrowing of the strong optical absorbance in the vicinity of 275 nm and suppression of the weaker absorbance at 400 nm with increasing temperature, suggesting a small shift in the occupancy of the e_g and t_{2g} orbitals. Based on earlier comparisons of theory, X-ray absorption, and optical absorption,⁴³ this 270 to 280 nm absorption band and 400 nm band correspond to excitations to unoccupied hybridized

We can identify unoccupied states, with both ligand and metal contributions, at 1.8 to 1.9 eV, 3.1 to 3.5 eV and 4.1 to 4.7 eV, as seen in Figure 3 and described elsewhere.⁴³ A comparison of the largely metal-weighted XAS-derived unoccupied density of states (obtained by subtracting the core level binding energy from the XAS photon energy⁴³) with the inverse photoemission, which is very surface sensitive and thus probes largely the ligand related density of states, is illustrated in Figure 3.43 From the known symmetry of the unoccupied states, excitations to the unoccupied states at 1.8 to 1.9 eV above the Fermi level are forbidden by optical symmetry selection rules as the initial and final states are orthogonal, and thus not seen in optical absorption. For this reason, excitation to these low-lying states will not lead to an excited state that can readily decay to the HS state.⁴³ In contrast, excitations to the unoccupied states 3.1 to 3.5 eV and 4.1 to 4.7 eV, as seen in Figure 3, should lead to an occupied state that might decay to the HS state. 41,42 The characteristics of the temperature



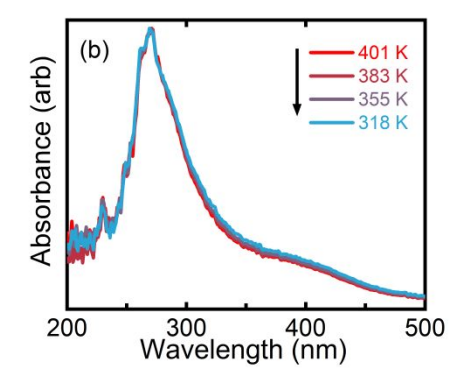


Figure 2. Temperature dependent UV-Vis spectra of a thin film of [Co(SQ)(Cat)(3-tpp)₂] on a glass substrate with initial increasing temperature (a) and subsequent decreasing temperature (b). During the temperature increase, a clear shift in the absorbance peak is observed. Upon decreasing the temperature, no change is observed. Intermediate temperature spectra have been omitted for visual clarity.

dependent UV-Vis measurement results agree with the data obtained using XAS and prior theoretical calculations of the electronic structure. The optical absorption features at 290 nm represent photon wavelengths close to the combined unoccupied ligand (at about 4.7 eV seen in inverse

photoemission) and metal state binding energies (corresponding to a feature at 4.1 eV above the threshold edge, in X-ray absorption). As with the X-ray absorption spectra (supplementary materials), the optical absorption spectrum, seen at 400 K, is then largely preserved on the subsequent decrease in sample temperature (Figure 2). This is consistent with a persistent excitation to the HS $[Co(SQ)_2(3-tpp)_2]$ tautomer, independent of temperature.

The weak 400 nm optical absorption band (Figure 2) corresponds to excitations to a strong Co-weighted unoccupied state observed in X-ray absorption (Figure 3a and supplementary materials) at 3.1 eV and as ascertained from the matching spectral weight in the inverse photoemission, contains weak ligand contributions (Figure 3b). This excitation is metal weighted state, with both ligand and metal unoccupied orbital contributions in the HS state, but for which optical excitations are largely, but not completely, forbidden (hence weak in optical absorption). The energy of this ligand plus metal unoccupied state correlates with the wavelength dependence of the temperature and optical illumination enhanced conductance changes discussed below.

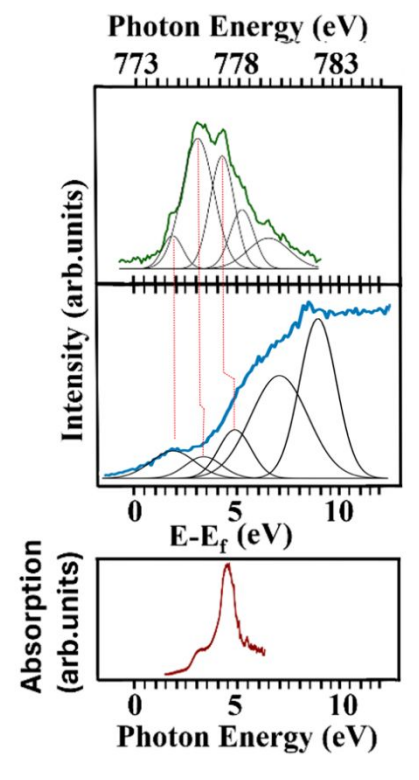


Figure 3. A comparison of the unoccupied states of $[Co(SQ)(Cat)(3-tpp)_2]/[Co(SQ)_2(3-tpp)_2]$ thin films through various spectroscopies. a) The Co $2p_{3/2}$ X-ray absorption spectra of $[Co(SQ)(Cat)(3-tpp)_2]/[Co(SQ)_2(3-tpp)_2]$ at 300 K, b) the unoccupied states from inverse photoemission $[Co(SQ)(Cat)(3-tpp)_2]/[Co(SQ)_2(3-tpp)_2]$ thin films at 300 K deposited on a polyaniline molecular layer, c) the UV-VIS absorption spectra of $[Co(SQ)(Cat)(3-tpp)_2]/[Co(SQ)_2(3-tpp)_2]$ at 300 K. The components from XAS of $[Co(SQ)(Cat)(3-tpp)_2]/[Co(SQ)_2(3-tpp)_2]$ has been lined up with the approximated components of inverse photoemission spectra and absorption spectra.

Conductance Changes with Temperature and Optical Excitation

Conductance studies suggests that visible-light illumination allows toggling between conductance states at elevated temperatures. To further investigate the photo-active conductance response of [Co(SQ)(Cat)(3-tpp)₂], light and temperature dependent electronic transport measurements were performed on the sample at variable temperatures and light sources with the bias voltage ramping typically between ±1.4 V. The resulting conductance measurements exhibited intricate interdependence among the bias voltage, the irradiation wavelength, and the annealing history of the sample.

Figure 4a shows the conductivity of a sample as a function of temperature while under total darkness (without any light irradiation). The conductivity exhibited robustly reproducible behaviour, with increasing and decreasing temperature cycles, but with an overall decrease in conductivity with increasing temperature, in the absence of illumination. This behaviour is distinct from the abrupt changes in conductivity discussed below. In spite of the low conductivity, the conductivity is close to a linear decrease with increasing temperature, which somewhat resembles a metal and may be the result of a significant density of states predicted, by density functional theory, at the Fermi level.⁴³ This indicates that there is no abrupt conductance transition associated with temperature change, over a wide range in temperature where the valence tautomeric change in the spin state occurs, 43 if there is no light irradiation. Multiple repeated measurements were conducted without photon excitation and under illumination from various colours of light on the sample. The measurements in the absence of illumination or with illumination with red light showed identical results and confirm that a significant conductance transition does not happen even well above 370 K, as summarized in Figures 4a and 4b.

In the presence of light of shorter wave lengths, abrupt changes in conductivity are seen. Figure 4c shows the temperature dependent I(V) data of the sample irradiated by incandescent (broad spectrum) light. In this instance, the sample conductance starts in a generally lower conductive state, as shown by the green curve of Figure 4c, obtained at 333 K. As the temperature increased to 373 K, the conduction current jumped to a higher value at a bias voltage of around 1.25 V, as shown by the red curve in Figure 4c, in the presence of illumination. The now higher conductance then remained stable even after decreasing temperature, as shown by the blue curve in Figure 4c. We also observed that changes in the conductivity occur in the vicinity of 360 K to 370 K at the higher electric field (higher bias voltages), and the higher conductance state of [Co(SQ)₂(3-tpp)₂] is more robustly retained, as seen in Figure 4d.

Based on multiple I(V) curves, we extracted the conductivity as a function of temperature at a bias voltage of 1.25 V, and the data are summarized in Figure 4d, with the temperature history indicated by the arrows. With the initial heating, the conductivity of the sample increased abruptly by a factor of two,

at temperatures in the vicinity of \sim 370 K, with the combination of visible-light illumination and an applied voltage.

The temperature dependence tends to implicate the tautomeric transition or change in spin plays a role in this abrupt

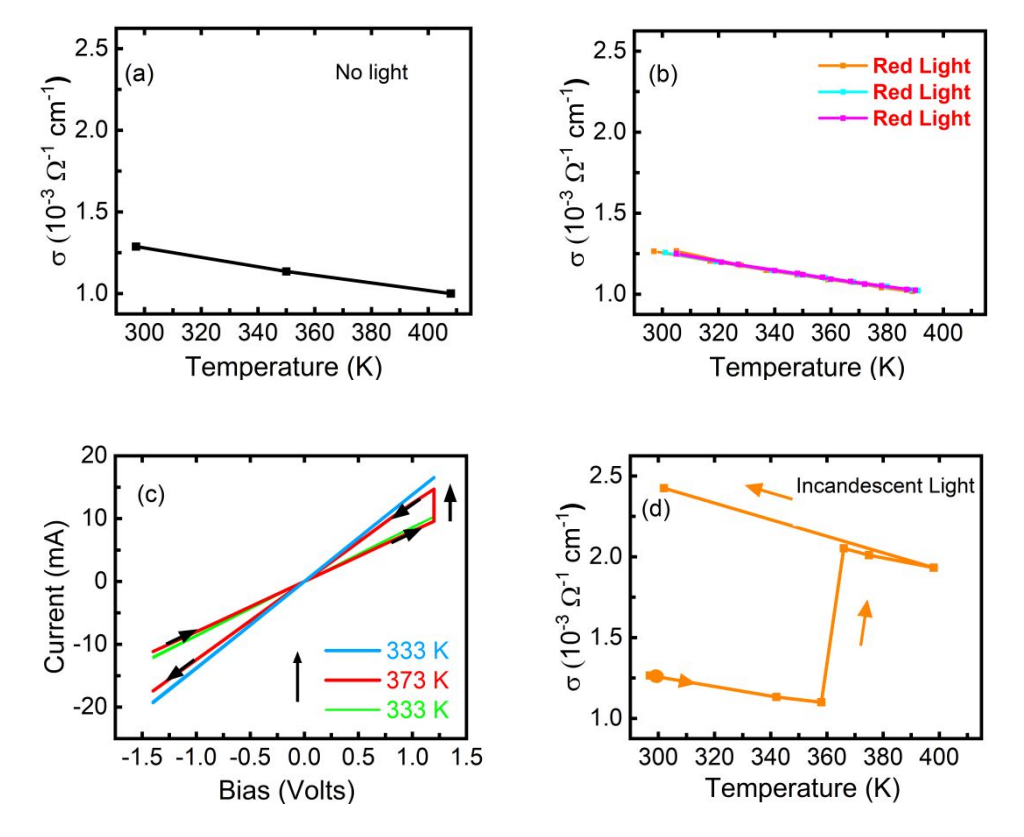


Figure 4. The temperature, light, and bias dependent electric transport measurements of [Co(SQ)(Cat)(3-tpp)₂] thin films. (a) The temperature dependent conductivity plot of a sample measured in darkness. (b) The conductivity data of the sample for 3 cycles measured when the sample was illuminated by a red LED. (c) I(V) data of a sample measured at different temperatures under incandescent light irradiation. (d) The temperature dependent conductivity plot (with a bias voltage of 1.25 V) as a function of temperature while the sample was held under incandescent light.

This higher conductance state was retained with decreasing temperature, although, as before, conductance surprisingly increases with decreasing temperature (though at a much higher overall conductance). The initial conductance change is consistent with both the XAS (supplementary materials) and UV-Vis data (Figure 2) that also suggest that thin films of [Co(SQ)(Cat)(3-tpp)₂] indeed undergo a valence tautomeric spin transition near 370 K, consistent with the magnetometry of prior work. The locking in the high conductance state on raising the temperature above 360 K (Figure 4d) is also consistent with effects of continued illumination as seen in both the optical absorption and XAS, as discussed above.

Magnetometry measurements indicate that $[Co(SQ)(Cat)(3-tpp)_2]$ undergoes a gradual valence tautomeric transition from the LS to HS state when the sample is heated from 300 K to 400 K, with the midpoint of the conversion occurring around 370 K, as seen in the supplementary materials Figure S4. ^{43,44} In this context, the prevalence of conduction changes near the transition temperature of 370 K is thought to be significant. The physical re-organization of molecules could also contribute to the conductance change as could be the tautomeric spin state transition and excitations to an excited state like the ligand to metal change transfer state.

change in conductance. Yet the change in conductance remains stable with decreasing temperature, and neither the XAS nor the optical absorption change significantly with temperature indicating that under illumination, the [Co^{II}(SQ)₂(3-tpp)₂] high spin state is favoured. With the physical re-organization of molecules, one would expect some partial changes in conductance, rather than the discrete change in conductance seen here, as the physical re-organization of molecules cannot always be a complete process for the entire film. This latter effect is not seen. Yet, we can completely exclude either the tautomeric transition or change in spin or a physical reorganization of molecules as playing a role in the mechanism for conductance change. Yet the wavelength dependence of the illumination necessary for the conductance change and reversibility of the conductance change implicates the ligand to metal change transfer state (LMTS), discussed above, as playing a significant role.

It seems very plausible that this conductance switching and then "locking" in the high conductance state is associated with optical excitations to the LMCT and ligand-centered excited states, as such conductance switching is only observed in the presence of illumination that contains short wavelength (higher energy photons), as seen in Figures 4c and 4d. The absence of

conductance switching in the presence of illumination at longer wavelengths in the vicinity of 600 nm (Figure 4b), or much longer wavelengths (lower energies) than any of the optical absorption features is believed to be significant. The fact that conductance does not change, at temperatures associated with the valence tautomeric transition and in the absence of illumination by short wavelength light, suggests sustained occupancy of the LMCT and ligand-centered excited states are required for the abrupt conductance changes. As noted above, optical excitations to the low-lying unoccupied states at 1.8 to 1.9 eV above the Fermi level, noted above, are not favoured, again consistent with the observation that longer wavelength illumination does not lead to an observed conductance change.

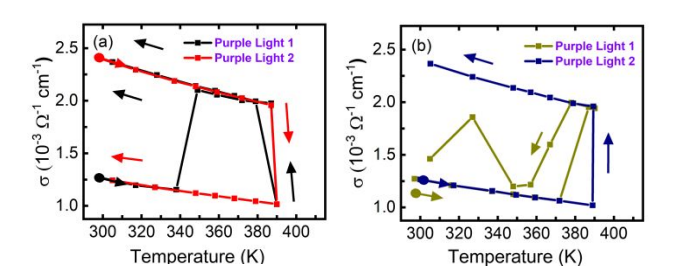


Figure 5. The temperature dependent conductivity of [Co(SQ)(Cat)(3-tpp)₂] thin films under illumination with a purple LED on an interdigitated electrode template. (a) The temperature dependent conductivity of a sample while illuminated by a violet LED for the first 2 cycles. (b) The temperature dependent conductivity plots of the sample during later annealing cycles. Throughout, the sample is illuminated by a violet LED and the bias voltage is 1.25 V.

To demonstrate that the observed conductance switching represents bistability for the tautomers Co(SQ)(Cat)(3 $tpp)_2]/[Co(SQ)_2(3-tpp)_2]$, we performed the same electric transport measurements using a violet LED light source (380 to 420 nm), as well as with a small applied electric field of 1.25 V. The I(V) measurements were carried out for a sample first illuminated by a violet LED light source during the temperature ramping up process followed by temperature ramping down. We repeated the cycles, with the conductivity data extracted from I(V) curves summarized in Figure 5a. The initial annealing and colling temperature cycle (labeled as the black curve with arrows denoting the temperature ramping directions) begins with a low conductivity state, similar to Figure 4d, however, the conductance is seen to flip between the high and low conductance states as the temperature increases, and finally stabilizing in the higher conductivity state when the temperature approaches 390 K. As the temperature is ramped back down to room temperature and the spin state is seen to be stabilized in the higher conductance state. But this conductance switching is clearly reversible as with a second annealing cycle (indicated by the red curve in Figure 5a) the conductance transitions back to the lower conductance state as the temperature increases to 390 K, and then stabilizes now in the lower conductance state with decreasing temperature. This phenomenon of switching back and forth between two very different conductance values while under violet LED

illumination, and a bias voltage of 1.25 V, was observed in multiple samples and is persistent under many annealing cycles, as indicated in Figure 5. The sample's conductivity typically "switches" at temperatures near 370 K to 390 K, retaining a characteristic higher or lower conductance, until the temperature is ramped again, and then may "switches" again. The switching of the conductance near the spin state transition temperature, then locking "in" lower conductance, while the overall conductance continues to increase with decreasing temperature is unusual but not unprecedented having been seen for the spin crossover complex [Fe(III)(3-OMe-Sal₂trien))][Ni(dmit)₂].⁴⁸

Decreasing the photon energy from roughly 3 eV (violet) to 2 eV (red) results in the loss of the significant temperature dependent conductance switching, adopting behaviour of that in Figure 4b. A subsequent increase in photon energy back to roughly 3 eV (violet) restores the conductance switching as seen in Figure 5b with repeated cycles of measurements. This indicates that this conductance switching for the valence tautomers [Co(SQ)(Cat)(3-tpp)₂]/[Co(SQ)₂(3-tpp)₂] depends not only on temperature but the photon energy used in illumination, and that the conductance switching is reversible. While the temperature dependence does some suggest a possible role tautomeric transition the photon energy dependence tends to suggest that conductance switching does not occur without some charge population occupying the normally unoccupied ligand-metal charge transfer LMCT states.

Evidence of Voltage Effects on the Conductance Changes

Not only is the conductance switching observed to repeatedly occur when the temperature is close to the tautomeric spin state transition temperature of 370 K (Figure 5) but toggling between the higher and lower conductance state occurs with bias voltage sweeps as the temperature is increased, as shown in Figure 6a. The initial I(V) data, taken at a temperature of 300 K (orange line in Figure 6a), has a maximum current around 7.5 mA at a bias voltage of 1.5 V and exhibits no conductance switching with bias voltage. As the temperature is increased, the conductance of the [Co(SQ)(Cat)(3 $tpp)_2]/[Co(SQ)_2(3-tpp)_2]$ thin film hops between two characteristic I(V) slopes, for the data taken at 360 K and 385 K (Figure 6a). At the elevated temperature of 390 K, the conductance of the $[Co(SQ)(Cat)(3-tpp)_2]/[Co(SQ)_2(3-tpp)_2]$, and in the example of Figure 6a, stabilizes in the high conductance state, as evident in the toggling between the two conductance states as the voltage is raised from 0 V bias to 1.5 V, but with diminished conductance changes as the voltage is decreased to -1.5 V. The stability of the high conductance persists as the temperature is reduced back to 300 K, with a maximum current around 15 mA at the bias voltage of 1.5 V, different from the initial low conductance state.

These observations do not exclude the possibility that the conductance fluctuations with temperature and light are aided by the bistability between the low spin [Co(SQ)(Cat)(3-tpp)₂]

and the high spin $[Co(SQ)_2(3-tpp)_2]$ states, as has been seen with other spin crossover molecular systems.⁴⁹ While it is observed that the conductance toggles between the initial low conductance state and a higher conductance state, when the temperature is close to the tautomeric spin state transition temperature of 370 K it is also significant that the [Co(SQ)₂(3tpp)2] thin film can stabilize in either a high or low conductance state when reducing the temperature well below the tautomeric spin state transition temperature of 370 K. This supports the thesis that charge trapping may also play a role, as indicated by the changes in conductance with voltage sweeps near the tautomeric spin state transition temperature of 370 K. So if the ground state energies in both the low spin $[Co(SQ)(Cat)(3-tpp)_2]$ and the high spin $[Co(SQ)_2(3-tpp)_2]$ states are comparable, as illustrated in Figure 6b, either state can be stabilized after the switching by either charge trapping or population of the normally unoccupied ligand-metal charge transfer states. The relaxation time from one state to the other state is long (several days based on our observations) but the population of the normally unoccupied ligand-metal charge transfer states facilitates the transition between conductance states since temperature alone has little effect (Figure 4).

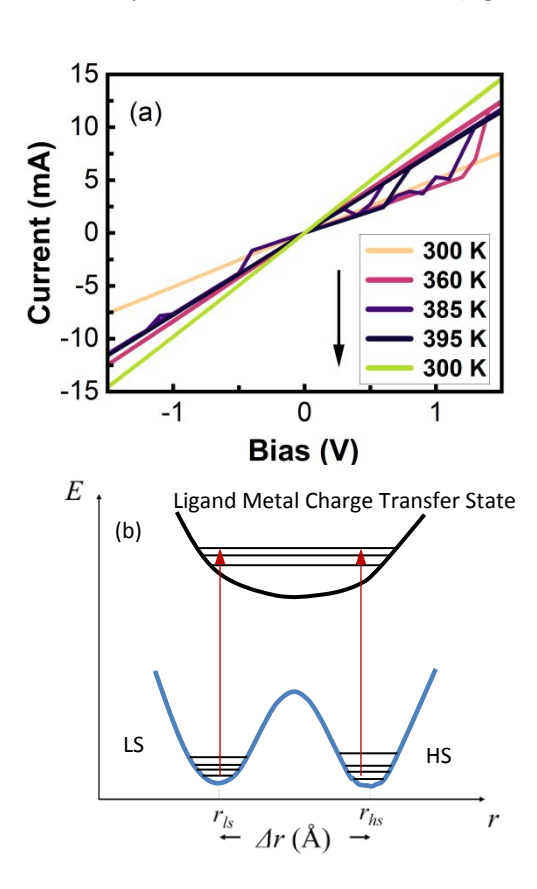


Figure 6. (a) The I(V) data of a sample measured at different temperatures illuminated by white light, the temperature was increased from 300 K to 395 K and then cooled down back to 300 K. The data taken at 360 K and 385 K which is near the transition temperature showing the "hopping" between two conductance values (some intermediate temperature data have been omitted for clarity). (b)The schematic energy diagram of LS and HS states with comparable energies.

Deterministic Switching

As indicated above, changing the applied voltage to $[Co(SQ)(Cat)(3-tpp)_2]/[Co(SQ)_2(3-tpp)_2]$ by itself does not necessarily lead to deterministic switching. The role of the substrate, nonethelss, cannot be ignored. The substrate does have an effect on the tautomeric/spin state of [Co(SQ)(Cat)(3tpp)2]/[Co(SQ)2(3-tpp)2] thin films, and this can provide for voltage control of the state. As seen in Figure 7, the optical absorption of a $[Co(SQ)(Cat)(3-tpp)_2]/[Co(SQ)_2(3-tpp)_2]$ thin film the organic ferroelectric polyvinylidene fluoridehexafluoropropylene (PVDF-HFP) is surprisingly sensitive to the ferroelectric PVDF-HFP polarization is spite of the significant thickness of the [Co(SQ)(Cat)(3-tpp)₂]/[Co(SQ)₂(3-tpp)₂] thin film (300 nm). As with the spin crossover complex $[Fe\{H_2B(pz)_2\}_2(bipy)]$ (pz = tris (pyrazol-1-1y)-borohydride, bipy = 2,2'-bipyridine), the optical absorption depends on the electric polarization of the adjacent polymer ferroelectric polyvinylidene fluoride-hexafluoropropylene (PVDF-HFP).⁴⁷ Indeed, the changes in optical absorption seen here, in Figure 7 as a result of the changing polarization of the adjacent organic ferroelectric layer, are far more significant that observed in Figure 2. In Figure 7, the absorption feature at 270 nm is effectively quenched when the PVDF-HFP is polarized "down". This supports the contention that under normal circumstances the [Co(SQ)(Cat)(3-tpp)₂]/[Co(SQ)₂(3-tpp)₂] thin film remains largely in the high spin state under the optical fluence required for optical absorption.

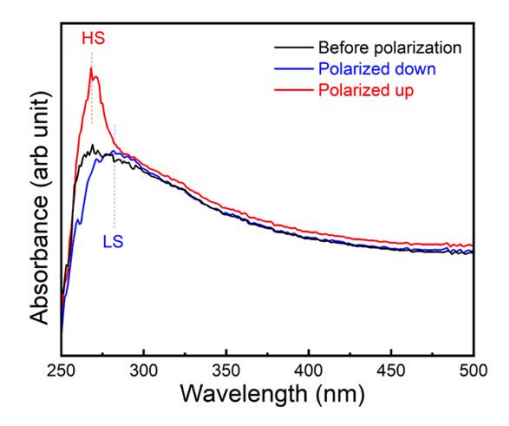


Figure 7. The room temperature UV-Vis spectra of the bilayer PVDF-HFP (25 layers)/ $[Co(SQ)(Cat)(3-tpp)_2]/[Co(SQ)_2(3-tpp)_2]$ thin films (300 nm) samples. The PVDF-HFP layers were polarized toward different directions.

Since the ferroelectric polarization of the PVDF-HFP layer can be switched through an applied voltage and the state of the $[Co(SQ)(Cat)(3-tpp)_2]/[Co(SQ)_2(3-tpp)_2]$ thin film depends on the direction of the PVDF-HFP polarization, we must conclude that deterministic switching of $[Co(SQ)(Cat)(3-tpp)_2]/[Co(SQ)_2(3-tpp)_2]$ thin film electronic structure is realizable.

Conclusions

While conductance changes, for spin crossover complexes, as a result of changing illumination, has been reported

previously, 50,51 and an applied electric field is known to affect the bistability, 19,52 the effect of the combination of light and applied field on conductance has not, hitherto, been given the attention it deserves. In this study, we reported the temperature dependent spin transition exhibited [Co(SQ)(Cat)(3-tpp)₂] molecules under different light irradiation conditions. Clearly, for [Co(SQ)(Cat)(3-tpp)₂]/[Co(SQ)₂(3-tpp)₂], the conductance changes are activated by a combination of both photo-excitations and temperature, and it is also sensitive to the electric field. When the temperature is close to the transition temperature, a photon with energy above a certain threshold is required to switch the conductance state, and the conductance may initially not appear stable. Yet under illumination and voltage, either the high or low conductance state can be stabilized upon reducing the [Co(SQ)(Cat)(3tpp)₂]/[Co(SQ)₂(3-tpp)₂] thin film sample temperature from an elevated temperature at or above 370 K to room temperature. This indicates that the low and high conductance states likely have relatively comparable energy, and yet the activation energy to switch the conductance is reasonably high, thus leading to an extensive, long relaxation time, or requires sustained illumination. The [Co(SQ)(Cat)(3-tpp)₂] molecules demonstrate light induced bistability, 42,47 but here, a change in spin state is not necessarily implicated. Without question, we have demonstrated an interplay between the occupation of the ligand-metal charge transfer state, the [Co(SQ)(Cat)(3 $tpp)_2]/[Co(SQ)_2(3-tpp)_2]$ and the conductance of the $[Co(SQ)(Cat)(3-tpp)_2]/[Co(SQ)_2(3-tpp)_2]$ thin films.

Author contributions

J. P.: sample preparation, data curation, data analysis, software, and writing-original draft; S. Y.: sample preparation, data curation, data analysis, and writing-review & editing; J. S.: sample preparation, data curation, and software; J. O.: sample preparation, data curation, and editing draft; T. E.: data curation; E. M.: data curation; P. W.: molecules synthesis; M. Z.: data curation; J. L.: funding acquisition, and editing draft; A. N.: data curation, M. S.: conceptualization, review and editing; P. A. D. conceptualization, funding acquisition, methodology, and writing-review & editing; R. H.: conceptualization, funding acquisition, methodology, project administration, and writing-review & editing.

Conflicts of interest

There are no conflicts to declare.

Acknowledgements

This research was supported by the National Science Foundation through NSF-DMR 2317464 [Jared P. Phillips, Saeed Yazdani, Joseph Soruco, Jackson Oles, Thilini K. Ekanyaka, Esha Mishra, M. Zaid Zaz, Peter A. Dowben, Ruihua Cheng] and Purdue University Center for Quantum Technologies [Joseph Soruco, Jing Liu]. Use of the Advanced Light Source, Lawrence Berkeley National Laboratory, was supported by the U.S. Department of Energy (DOE) under contract DE-AC02-05CH11231. The synthesis and characterization of the $[Co(SQ)(Cat)(3-tpp)_2]/[Co(SQ)_2(3-tpp)_2]$

complex was carried out by the Shatruk group as part of research within the Center for Molecular Magnetic Quantum Materials, an Energy Frontier Research Center funded by the U.S. Department of Energy, Office of Science, Basic Energy Sciences under Award no. DESC0019330. Multiple discussions with Talat Rahman and Duy Le are gratefully acknowledged.

References

- 1 L. Cambi and L. Szegö, "Über Die Magnetische Susceptibilität Der Komplexen Verbindungen", Ber. Dtsch. Chem. Ges., A/B, 1931, **64**, 2591. https://doi.org/10.1002/cber.19310641002
- L. Cambi and L. Malatesta, "Magnetismus Und Polymorphie Innerer Komplexsalze: Eisensalze Der Dithiocarbamidsäuren", Ber. Dtsch. Chem. Ges. A/B, 1937, 70, 2067. https://doi.org/10.1002/cber.19370701006
- W. A. Baker and H. M. Bobonich, "Magnetic Properties of Some High-Spin Complexes of Iron(II)", Inorg. Chem., 1964, 3, 1184. https://doi.org/10.1021/ic50018a027
- A. Cornia and P. Seneor, "The Molecular Way", Nature Mater., 2017, 16, 505.
 - https://doi.org/10.1038/nmat4900
- P. Gütlich, Y. Garcia, and H. A. Goodwin, "Spin Crossover Phenomena in Fe(II) Complexes", Chem. Soc. Rev., 2000, 29, 419-427. https://doi.org/10.1039/B003504L
- P. Gütlich and H. A. Goodwin, "Spin Crossover in Transition Metal Compounds II", Vol. 234 (Springer Berlin Heidelberg, Berlin, Heidelberg, 2004). https://doi.org/10.1007/b93641
- M. Shatruk, H. Phan, B. A. Chrisostomo, and A. Suleimenova, "Symmetry-Breaking Structural Phase Transitions in Spin Crossover Complexes", Coordination Chemistry Reviews, 2015, **289**, 62. https://doi.org/10.1016/j.ccr.2014.09.018
- 8 O. Sato, "Dynamic Molecular Crystals with Switchable Physical Chem., Properties". Nat. 644-656. 2016, https://doi.org/10.1038/nchem.2547.
- N.A.A.M. Amin, S.M. Said, M.F.M. Salleh, A.M. Afifi, N.M.J.N. Ibrahim, M.M.I.M. Hasnan, M. Tahir, N.Z.I. Hashim, "Review of Fe-based spin crossover metal complexes in multiscale device architectures", Inorganica Chimica Acta, 2023, 544,121168.
 - https://doi.org/10.1016/j.ica.2022.121168
- 10 T. K. Ekanayaka, G. Hao, A. Mosey, A. S. Dale, X. Jiang, A. J. Yost, K. R. Sapkota, G. T. Wang, J. Zhang, A. T. N'Diaye, A. Marshall, R.C. Cheng, A. Naeemi, X.S. Xu, and P.A. Dowben, "Nonvolatile Voltage Controlled Molecular Spin-state Switching for Memory Applications". Magnetochemistry, 2021, 7(3), 37.
 - https://doi.org/10.3390/magnetochemistry7030037.
- 11 K. S. Kumar and M. Ruben, "Sublimable Spin-Crossover Complexes: From Spin-State Switching to Molecular Devices", Ed. 2021, 60, 7502-7521. Chem. Int. https://doi.org/10.1002/anie.201911256
- 12 G. Hao, A. Mosey, X. Jiang, A. J. Yost, K. R. Sapkota, G. T. Wang, X.; Zhang, J. Zhang, A. T. N'Diaye, R. C. Cheng, X.S. Xu, and P.A. Dowben, "Nonvolatile Voltage Controlled Molecular Spin State Switching", Appl. Phys. Lett., 2019, 114 (3), 032901. https://doi.org/10.1063/1.5054909.
- 13 C. Lefter, R. Tan, S. Tricard, J. Dugay, G. Molnár, L. Salmon, J. Carrey, A. Rotaru, and A. Bousseksou, "On the stability of spin crossover materials: From bulk samples to electronic devices", Polyhedron, 2015, 102. 434-440.https://doi.org/10.1016/j.poly.2015.10.021
- 14 C. Lefter, V. Davesne, L. Salmon, G. Molnár, P. Demont, A. Rotaru, and A. Bousseksou, "Charge Transport and Electrical Properties of Spin Crossover Materials: Nanoelectronic and Spintronic Devices", Magnetochemistry, 2016, 2, 18

- doi:10.3390/magnetochemistry2010018
- 15 J. Dugay, M. Giménez-Marqués, T. Kozlova, H. W. Zandbergen, E. Coronado, and H. S. J. van der Zant, "Spin Switching in Electronic Devices Based on 2D Assemblies of Spin-Crossover Nanoparticles." Advanced Materials, 2015, 27, 1288-1293.
 - https://doi.org/10.1002/adma.201404441
- 16 L. Salmon, G. Molnár, S. Cobo, P. Oulié, M. Etienne, T. Mahfoud, P. Demont, A. Eguchi, H. Watanabe, K. Tanaka, and A. Bousseksou, "Re-investigation of the spin crossover phenomenon in the ferrous complex [Fe(HB(pz)₃)₂]", *New J. Chem.*, 2009, **33**, 1283-1289. https://doi.org/10.1039/B902811K
- 17 A. Rotaru, I. A. Gural'skiy, G. Molnár, L. Salmon, P. Demont, and A. Bousseksou, "Spin state dependence of electrical conductivity of spin crossover materials", *Chem. Commun.*, 2012, 48, 4163-4165. https://doi.org/10.1039/C2CC30528C
- 18 C. Lefter, I. A. Gural'skiy, H. Peng, G. Molnár, L. Salmon, A. Rotaru, A. Bousseksou, and P. Demont, "Dielectric and charge transport properties of the spin crossover complex [Fe(Htrz)₂(trz)](BF₄)", *Physica Status Solidi* (RRL), 2014, **8**, 191-193.
 - http://dx.doi.org/10.1002/pssr.201308256
- 19 A. Rotaru, J. Dugay, R. P. Tan, I. A. Gural'skiy, L. Salmon, P. Demont, J. Carrey, G. Molnár, M. Respaud, and <u>A.</u> Bousseksou, "Nano-electromanipulation of Spin Crossover Nanorods: Towards Switchable Nanoelectronic Devices." *Adv. Mater.*, 2013, **25**, 1745. http://dx.doi.org/10.1002/adma.201203020
- 20 A. Mosey, A. S. Dale, G. Hao, A. N'Diaye, P. A. Dowben, R. Cheng, "Quantitative Study of Energy Change in Voltage-controlled Spin Crossover Molecules for Molecular Spintronics", *J. Phys. Chem. Lett.*, 2020, **11**, 8231–8237. https://doi.10.1021/acs.jpclett.0c02209
- 21 F. Prins, M. Monrabal-Capilla, E. A. Osorio, E. Coronado, H. S. J. van der Zant, "Room-temperature electrical addressing of a bistable spin-crossover molecular system", Advanced Materials, 2011, 23, 1545-1549. https://doi.org/10.1002/adma.201003821
- 22 M. Wang, Z. Li, R. Ishikawa, and M. Yamashita, "Spin crossover and valence tautomerism conductors", *Coordination Chemistry Reviews*, 2021, **435**, 213819 https://doi.org/10.1016/j.ccr.2021.213819
- 23 D. A. Shultz, "Valence Tautomerism in Dioxolene Complexes of Cobalt". *Magn. Mol. Mater. II Models Exp.* 2001, 281306. https://doi.org/10.1002/3527600590.ch8
- 24 T. Tezgerevska, K. G. Alley, and C. Boskovic, "Valence Tautomerism in Metal Complexes: Stimulated and Reversible Intramolecular Electron Transfer between Metal Centers and Organic Ligands", Coord. Chem. Rev. 2014, 268, 23-40. https://doi.org/10.1016/j.ccr.2014.01.014
- 25 R. D. Schmidt, D. A. Shultz, J. D. Martin and P. D. Boyle, *J. Am. Chem. Soc.*, 2010, **132**, 6261–6273. https://doi.org/10.1021/ja101957c
- 26 D. M. Adams, A. Dei, A. L. Rheingold, and D. N. Hendrickson, "Bistability in the [Co^{II} (Semiquinonate)₂] to [Co^{III} (Catecholate)(Semiquinonate)] Valence-Tautomeric Conversion", *J. Am. Chem. Soc.* 1993, **115** (18), 8221-8229. https://doi.org/10.1021/ja00071a035
- 27 D. N. Hendrickson, and C. G. Pierpont, "Valence Tautomeric Transition Metal Complexes", in: Spin Crossover in Transition Metal Compounds II", *Topics in Current Chemistry*, vol **234**, pp. 63–95; Springer, Berlin, Heidelberg. https://doi.org/10.1007/b954132012, https://doi.org/10.1007/b95413.
- 28 C. Roux, D. M. Adams, J. P. Itié, A. Polian, D. N. Hendrickson, and M. Verdaguer, "Pressure-Induced Valence Tautomerism

- in Cobalt o-Quinone Complexes: An x-Ray Absorption Study of the Low- Spin [Coll (3, 5-Dtbsq)(3, 5-Dtbcat)(Phen)] to High-Spin [Coll (3, 5-Dtbsq)₂(Phen)] Interconversion", *Inorg. Chem.* 1996, **35** (10), 2846-2852.
- https://doi.org/10.1021/ic951080o
- 29 J. Tao, H. Maruyama, O. Sato, "Valence Tautomeric Transitions with Thermal Hysteresis around Room Temperature and Photoinduced Effects Observed in a Cobalt-Tetraoxolene Complex". J. Am. Chem. Soc. 2006, 128 (6), 1790-1791. https://doi.org/10.1021/ja057488u
- 30 O. Sato, A. Cui, R. Matsuda, J. Tao, and S. Hayami, "Photo-Induced Valence Tautomerism in Co Complexes". *Acc. Chem. Res.* 2007, **40** (5), 361-369. https://doi.org/10.1021/ar600014m.
- 31 R. D. Schmidt, D. A. Shultz, and J. D. Martin, "Magnetic Bistability in a Cobalt Bis(Dioxolene) Complex: Long-Lived Photoinduced Valence Tautomerism", *Inorg. Chem.* 2010, **49** (7), 3162–3168. https://doi.org/10.1021/ic901998p.
- 32 R. D. Schmidt, D. A. Shultz, J. D. Martin, and P. D. Boyle, "Goldilocks Effect in Magnetic Bistability: Remote Substituent Modulation and Lattice Control of Photoinduced Valence Tautomerism and Light-Induced Thermal Hysteresis", *J. Am. Chem. Soc.* 2010, 132 (17), 6261–6273. https://doi.org/10.1021/ja101957c
- 33 C. Boskovic, "Valence Tautomeric Transitions in Cobalt-dioxolene Complexes", chapter 7 in Spin-Crossover Materials: Properties and Applications, First Edition. Edited by Malcolm A. Halcrow, 2013, John Wiley & Sons, Ltd. Published 2013 by John Wiley & Sons, Ltd.
- 34 O. Sato, S. Hayami, Z. Gu, K. Seki, R. Nakajima, and A. Fujishima, "Photo-Induced Long-Lived Intramolecular Electron Transfer in a Co Valence Tautomeric Complex", Chem. Lett. 2001, **30** (9), 874-875. https://doi.org/10.1246/cl.2001.874
- 35 D. M. Adams, B. Li, J. D. Simon, and D. N. Hendrickson, "Photoinduced Valence Tautomerism in Cobalt Complexes Containing Semiquinone Anion as Ligand: Dynamics of the High-Spin [Co^{II}(3,5-Dtbsq)₂] to Low-Spin [Co^{III}(3,5-Dtbsq)(3,5-Dtbcat)] Interconversion", *Angew. Chem. Int. Ed. Engl.* 1995, **34**), 1481.
 - https://doi.org/10.1002/anie.199514811.
- 36 J. Dai, S. Kanegawa, Z. Li, S. Kang, and O. Sato, "A Switchable Complex Ligand Exhibiting Photoinduced Valence Tautomerism". *Eur. J. Inorg. Chem.*, 2013, (24), 4150-4153. https://doi.org/10.1002/ejic.201300531.
- 37 G. Poneti, M. Mannini, L. Sorace, P. Sainctavit, M.-A. Arrio, A. Rogalev, F. Wilhelm, and A. Dei, "X-Ray Absorption Spectroscopy as a Probe of Photo- and Thermally Induced Valence Tautomeric Transition in a 1:1 Cobalt-Dioxolene Complex". *Chem. Phys. Chem.*, 2009, **10** (12), 2090-2095. https://doi.org/10.1002/cphc.200900098.
- 38 G. Poneti, M. Mannini, L. Sorace, P. Sainctavit, M.-A. Arrio, E. Otero, J. Criginski Cezar, and A. Dei, "Soft-X-Ray-Induced Redox Isomerism in a Cobalt Dioxolene Complex", *Angew. Chem. Int. Ed.*, 2010, **49** (11), 1954-1957. https://doi.org/10.1002/anie.200906895.
- 39 T. K. Ekanayaka, P. Wang, S. Yazdani, J. P. Phillips, E. Mishra, A. S. Dale, A. T. N'Diaye, C. Klewe, P. Shafer, J. Freeland, R. Streubel, J. P. Wampler, V. Zapf, R. Cheng, M. Shatruk, and P. A. Dowben, "Evidence of Dynamical Effects and Critical Field in a Cobalt Spin Crossover Complex", *Chem. Commun.* 2022, 58 (5), 661–664.
 - https://doi.org/10.1039/d1cc05309d.
- 40 T. M. Francisco, W. J. Gee, H. J. Shepherd, M. R. Warren, D. A. Shultz, P. R. Raithby, and C. B. Pinheiro, "Hard X-Ray-Induced Valence Tautomeric Interconversion in Cobalt-o-Dioxolene Complexes", J. Phys. Chem. Lett. 2017, 8 (19), 4774–4778. https://doi.org/10.1021/acs.jpclett.7b01794.

- 41 T. K. Ekanayaka, K. P. Maity, B. Doudin, and P. A. Dowben, "Dynamics of Spin Crossover Molecular Complexes" Nanomaterials, 2022, 12(10), 1742. https://doi.org/10.3390/nano12101742
- 42 A. Hauser, "Light-Induced Spin Crossover and the High-Spin→Low-Spin Relaxation", in Spin Crossover in Transition Metal Compounds II, Vol. 234 (Springer Berlin Heidelberg, Berlin, Heidelberg, 2004), pp. 155−198. https://doi.org/10.1007/b95416
- 43 E. Mishra, T. K. Ekanayaka, T. Panagiotakopoulos, D. Le, T. S. Rahman, P. Wang, M. A. McElveen, J. P. Phillips, M. Z. Zaz, S. Yazdani, A. T. N'Diaye, R. Y. Lai, R. Streubel, R. Cheng, M. Shatruk, and P. A. Dowben, "Electronic structure of cobalt valence tautomeric molecules in different environments", Nanoscale, 2023, 15, 2044-2053. https://doi.org/10.1039/D2NR06834F
- 44 Ping Wang, Sandugash Yergeshbayeva, Xinsong Lin, Shubham Bisht, Miguel Gakiya-Teruya, and Michael Shatruk, "Structural and Magnetic Investigation of Cobalt Valence Tautomeric Complexes with Sulfur-Containing Ligands", Cryst. Growth Des. 2023, 23, 2384–2394; https://doi.org/10.1021/acs.cgd.2c01373
- 45 A. K. S. Kumar, Y. Zhang, D. Li, and R. G. Compton, "A Mini-Review: How Reliable Is the Drop Casting Technique?", *Electrochemistry Communications*, 2020, **121**, 106867. https://doi.org/10.1016/j.elecom.2020.106867
- 46 S. Yazdani, J. Phillips, T. K. Ekanayaka, P. Dowben, and R. Cheng, "The influence of the substrate on the functionality of spin crossover molecular materials", *Molecules* 2023, 28, 3735; https://doi.org/10.3390/molecules28093735
- 47 S. Yazdani, K. Collier, G. Yang, J. P. Phillips, A. S. Dale, A. Mosey, S. Grocki, J. Zhang, A. E. Shanahan, R. Cheng, and P. A. Dowben, "Optical characterization of isothermal spin state switching in an Fe(II) spin crossover molecular and polymer ferroelectric bilayer", J. Phys.: Condensed Matter., 2023, 35, 365401. doi: 10.1088/1361-648X/acd7ba
- 48 Yuri N. Shvachko, Nataliya G. Spitsyna, Denis V. Starichenko, Vladimir N. Zverev, Leokadiya V. Zorina, Sergey V. Simonov, Maksim A. Blagov and Eduard B. Yagubskii, "Magnetism, Conductivity and Spin-Spin Interactions in Layered Hybrid Structure of Anionic Radicals [Ni(dmit)₂] Alternated by Iron(III) Spin-Crossover Complex [Fe(III)(3-OMe-Sal₂trien)] and Ferric Moiety Precursors", Molecules 2020, 25, 4922; doi:10.3390/molecules25214922
- 49 P. Poganiuch, S. Decurtins, and P. Guetlich, "Thermal- and Light-Induced Spin Transition in [Fe(Mtz)₆](BF₄)₂: First Successful Formation of a Metastable Low-Spin State by Irradiation with Light at Low Temperatures", *J. Am. Chem. Soc.* 1990, **112**, 3270.
 - https://doi.org/10.1021/ja00165a003
- 50 C. Etrillard, V. Faramarzi, J. F. Dayen, J. F. Letard and B. Doudin, "Photoconduction in [Fe(Htrz)₂(trz)](BF₄)·H₂O nanocrystals", Chem. Commun., 2011, 47, 9663-9665. https://doi.org/10.1039/C1CC11441G
- 51 C. Lefter, R. Tan, J. Dugay, S. Tricard, G. Molnár, L. Salmon, J. Carrey, A. Rotaru, and A. Bousseksou, "Light induced modulation of charge transport phenomena across the bistability region in [Fe(Htrz)₂(trz)](BF₄) spin crossover microrods", *Phys. Chem. Chem. Phys.*, 2015,**17**, 5151-5154. https://doi.org/10.1039/C4CP05250A
- 52 C. Lefter, R. Tan, J. Dugay, S. Tricard, G. Molnár, L. Salmon, J. Carrey, W. Nicolazzi, A. Rotaru, and A. Bousseksou, "Unidirectional electric field-induced spin-state switching in spin crossover based microelectronic devices", *Chem. Phys. Lett.*, 2016, **644**, 138–141. http://dx.doi.org/10.1016/j.cplett.2015.11.036

Data Availability statement:

Raw data were generated at the Department of Physics research laboratory at Indiana University Indianapolis. Derived data supporting the findings of this study are available from the corresponding author R.C (email address rucheng@iu.edu) on request.